DOI: 10.1002/ejic.200800432

Synthesis and Characterization of $CoFe_2O_4$ Hollow Spheres

Yongde Meng,[a] Dairong Chen,*[a] and Xiuling Jiao[a]

Keywords: Nanostructures / Template synthesis / Magnetic materials / Mesoporous materials

$CoFe_2O_4$ hollow spheres with sizes ranging from 600 nm to 1 μm were prepared through hydrothermal treatment of an aqueous solution containing glucose, ammonium iron(II) sulfate hexahydrate [$(NH_4)_2Fe(SO_4)_2{\cdot}6H_2O$], and cobalt(II) sulfate heptahydrate [$CoSO_4{\cdot}7H_2O$], followed by calcination. The wall of the $CoFe_2O_4$ hollow spheres is composed of $CoFe_2O_4$ spinel nanoparticles with a size of ca. 30 nm and wall thickness of ca. 150 nm. Magnetic characterization indicates high coercivity and low saturation magnetization, which indicate potential applications as high-density magnetic recording materials and drug carriers.

Introduction

Owing to their low density, large specific surface area, hollow structure, and nanostructured wall, hollow spheres with nanometer or micrometer size often exhibit special physical and chemical properties different from solid particles. Hollow spheres have potential applications in many areas, such as optics, electrics, magnetics, medicine-release capsules, drug delivery, light-weight filler, selective adsorption, and catalysis.[1–4] Therefore, there has been great interest in preparing hollow structures with different compositions in recent years. In previous reports, the hollow spheres with nanocrystalline or amorphous shells were prepared through a variety of routes, among which the template routes including hard template and soft template methods were frequently applied. In the hard template process, a coating is formed first on the template (core) by controlled surface precipitation, and then the core is removed by thermal or chemical means to form hollow spheres. A variety of colloid particles such as silica particles, polystyrene spheres, carbon spheres, an so on have been used as hard templates to fabricate hollow spheres.[5–9] The hard template method has many advantages in the fabrication of hollow spheres: hollow spheres with different sizes can be achieved by the use of colloid particles of a given size, and the wall thickness and composition of hollow spheres can be controlled by adjusting reaction parameters. In the soft template technology, vesicles, micelles, and emulsions formed from amphiphilic molecules through self-assembly are often used as templates.[10–14] Soft templates are often in the nanometer-size range, and hollow spheres with nanometer sizes can be prepared through the soft template route. However, this approach has been limited because of the difficulty in controlling the size of the templates and the relatively harsh conditions required to form vesicles, micelles, and emulsions. Thus, there are more reports on the preparation of hollow spheres by the hard template method, in which carbon spheres are often used as a template to fabricate hollow spheres as a result of the rich functional groups on the surface. A large number of hollow spheres have been prepared by using carbon spheres as a template, mainly including oxides[15] and metal,[16] and the hydrothermal carbonization route has also been applied in the synthesis of metal/carbon nanocables and metal nanoparticles/carbon nanofiber composites.[17–19] However, there are few reports on hollow spheres composed of ternary metal oxides, because it is difficult to form a uniform coating of ternary oxides on the surface of the template. Here, $CoFe_2O_4$ core/shell precursor spheres are hydrothermally synthesized from a solution of metal oxide precursors and glucose, followed by calcination to form crystalline $CoFe_2O_4$ hollow spheres. In comparison with the two-step preparation of core/shell precursors in most reports, the $CoFe_2O_4$ core/shell precursor spheres are obtained through a one-pot synthesis. In addition, the formation mechanism of $CoFe_2O_4$ hollow spheres is proposed on the basis of experiments, and the magnetic properties were also investigated. As an important magnetic material, $CoFe_2O_4$ has high saturation magnetization, high coercivity, good mechanical hardness, and excellent chemical stability. In particular, its nanostructure has potential applications in many areas, including high-density magnetic recording, magnetic response imaging, and drug delivery among others.[20–24] Thus, it has attracted much interest in recent years and much research has focused on its preparation and magnetic properties. In previous reports, monodispersed $CoFe_2O_4$ nanoparticles[25–27] and $CoFe_2O_4$ nanowires[28,29] have been successfully prepared. However,

[a] School of Chemistry and Chemical Engineering, Shandong University,
Jinan 250100, P. R. China
E-mail: cdr@sdu.edu.cn

Supporting information for this article is available on the WWW under http://www.eurjic.org or from the author.

the preparation of magnetic hollow spheres mainly focused on Fe_3O_4 and α-Fe_2O_3.[30,31] In comparison, a magnetic ternary oxide such as $CoFe_2O_4$ exhibits relatively high thermal and chemical stability, which shows potential applications in many fields. Herein, $CoFe_2O_4$ hollow spheres were synthesized by the hydrothermal method. The objective of the present investigation is to prepare ternary oxide hollow spheres, which might exhibit novel or improved physical and chemical properties.

Results and Discussion

The product was obtained by hydrothermally treating an aqueous solution of glucose/cobalt sulfate/ammonium/iron(II) sulfate, followed by calcination. After hydrothermal treatment, the product was characterized by XRD. Upon examination of the XRD pattern, no crystalline peak can be observed, indicating that the hydrothermal sample is amorphous. After calcination, the XRD pattern of the product shows peaks at 2θ = 30.0, 35.4, 43.2, 53.4, 57.1, 62.6, 74.0, and all the diffraction peaks can be indexed to spinel $CoFe_2O_4$ (Figure 1; JCPDS No. 22–1086). The sharp diffraction peaks indicate the high crystallinity of the product. On the basis of on the (311) reflection, the lattice parameter is calculated to be a = 0.8404 nm, which is close to that of the bulk $CoFe_2O_4$ (a = 0.8395 nm). By using the Scherrer equation, the average size of the $CoFe_2O_4$ nanoparticles composing the hollow spheres is estimated to be ca.35 nm from the breadth of the (311) reflection. Due to the hollow structure of the product, X-rays can penetrate the sample and reach the glass sample holder during the XRD determination, and the amorphous scattering peak of the glass appears on the pattern. Then, a wide and low peak centered at ca. 23° can be observed excepting the sharp peaks of crystalline $CoFe_2O_4$. Energy dispersive X-ray spectroscopic (EDS) analysis shows that there are elements of Fe, Co, and O in the sample (Figure 2), and the atom ratio of cobalt to iron is 0.49, which is close to that of $CoFe_2O_4$. All the above analyses confirm that the sample is spinel $CoFe_2O_4$ without any impurities.

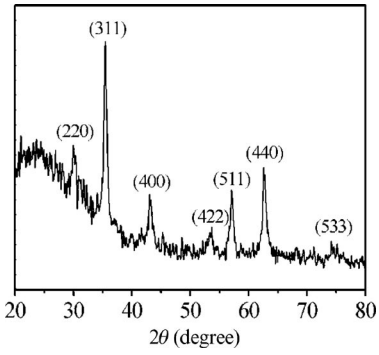

Figure 1. XRD pattern of $CoFe_2O_4$ hollow spheres.

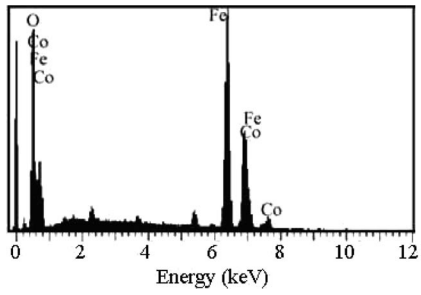

Figure 2. EDS of $CoFe_2O_4$ hollow spheres.

SEM and TEM images of the samples confirm their hollow structure. Both broken and unbroken hollow spheres can be observed (Figure 3a,b). The size of the $CoFe_2O_4$ hollow spheres ranges from 600 nm to 1 μm with a wall thickness of ca. 150 nm. The selected area electron diffraction (SAED) pattern shows a ring pattern, indicating that the nanocrystals comprised the cobalt ferrite hollow spheres aggregated disorderly, which is consistent with the HRTEM observation (Figure 3c). On the basis of the HRTEM image, the planar space of lattice fringes is about 0.48 nm, corresponding to the (111) plane of spinel $CoFe_2O_4$. On the basis of the HRTEM observation, the average size of the nanoparticles is ca. 30 nm, which is similar to that calculated from the XRD pattern (35 nm), and the slight difference may be because only a part of the particles could be observed during the HRTEM characterization. From the HRTEM image, pores can also be observed on the walls of the hollow spheres (denoted by the arrow in the Figure 3d), which is formed from the interparticle spacing of the nanocrystals. In addition, during the removal of carbon spheres by calcination, a large amount of carbon dioxide was released, also leading to pores in the shell.[32]

The N_2 adsorption–desorption curve shows a hysteresis loop in the relative pressure (P/P_0) range of 0.1–0.95 (Figure S1, Supporting Information) with a BET surface area of 74 m^2/g, indicating the presence of mesopores with a

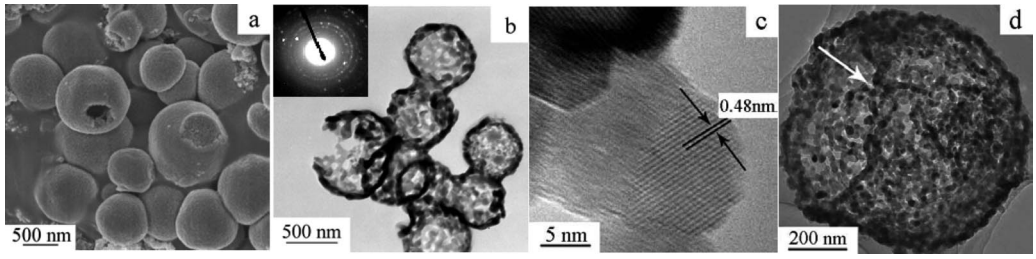

Figure 3. SEM (a), TEM (b), and HRTEM (c, d) images of $CoFe_2O_4$ hollow spheres; the inset in b is the SAED pattern of one $CoFe_2O_4$ hollow sphere.

broad pore size distribution in $CoFe_2O_4$ hollow spheres. This agrees well with the HRTEM observation.

The IR spectrum of the hydrothermal sample shows absorptions at 3397, 2915, 1695, 1616, 1300, 1107, 1013, 792, and 617 cm^{-1} (Figure S2, Supporting Information). The bands at 1616 and 3397 cm^{-1} are due to the adsorbed water. The absorptions at 2915 and 1107 cm^{-1} are attributed to the C–H and C–O vibrations from organic residues. The weak adsorptions at 1013, 792, and 617 cm^{-1} are attributed to SO_4^{2-}. The IR spectrum confirms the presence of sulfate, organics, and water in the hydrothermal sample. After calcination, the broad adsorption band at 581 cm^{-1} is attributed to the Fe–O vibration,[33] and the Co–O vibration cannot be observed due to the relatively low absorption wavenumbers. The absorption peaks at 2940 and 1105 cm^{-1} are attributed to the C–H and C–O vibrations from organic residues. The bands at 1622 and 3575 cm^{-1} are due to the adsorbed water. According to the relative intensity of the absorptions, it can be concluded that the hollow sphere is composed of $CoFe_2O_4$ with trace amounts of water and organics.

The TG curve of the hydrothermal sample exhibits a three-step weight loss from room temperature to 800 °C (Figure S3, Supporting Information). The first weight loss of 7.4% below 100 °C is attributed to the removal of the physically adsorbed water, and the second loss of ca. 2.6% from 100 to 280 °C results from the removal of the chemically adsorbed water. The main weight loss of 84.5% is attributed to the elimination of organic residue and the oxidation of the carbon templates between 280 and 480 °C. Further increasing the temperature to 800 °C, no other weight loss is detected, although the IR spectrum shows that there is a small amount of sulfate in the core/shell precursor. This discrepancy may be due to the fact that the amount of sulfate in the hydrothermal sample is too small to be detected by TG analysis. On the basis of TG analysis, the calcination temperature is set at 550 °C.

The XPS spectrum of $CoFe_2O_4$ hollow spheres shows signals for Co, Fe, and O in addition to the signal for the carbon reference. The O1s signal is located at 530.94 eV, and no other O1s level can be detected, which evidences the absence of impurities in the product. A $Co2p_{3/2}$ signal appears at 781.39 eV with a satellite peak at 786.65 eV; the peak at 796.89 eV is ascribed to the $Co2p_{1/2}$ level. The Fe2p level with binding energies of 711.61 and 725.04 eV is assigned to $Fe2p_{3/2}$ and $Fe2p_{1/2}$, respectively. The XPS result is in good agreement with the previous report,[34] and no obvious broadening can be observed for all the XPS peaks, indicating the phase-pure nature of the product (Figure 4).

In previous reports,[35] carbon spheres were often used as the template to synthesize hollow spheres. The process usually includes four steps: (1) preparation of the carbon spheres by hydrothermal carbonization, (2) separation of the carbon spheres from the mixture, (3) formation of the carbon/metal salt core–shell composite, and (4) removal of the carbon cores to form the hollow spheres. The group of Thomas prepared metal oxide hollow spheres by hydrothermal treatment of a glucose/metal salt mixture. After calcination, metal oxide hollow spheres were obtained. Their process is very simple.[36] In this paper, $CoFe_2O_4$ hollow sphere was prepared by hydrothermal treatment of a glucose/cobalt sulfate/ammonium iron(II) sulfate mixed solution. First, the carbon spheres were formed by a hydrothermal process. Due to the abundant number of hydroxy groups on the surface of the carbon spheres, the Co^{2+} and Fe^{2+} cations could be adsorbed onto them, thus forming an amorphous composite shell rather than a crystalline coating from heterogeneous nucleation, which was confirmed by XRD analysis. In the subsequent calcination process, the adsorbed water and organics as well as the carbon core were removed, and the crystalline $CoFe_2O_4$ hollow spheres were formed.

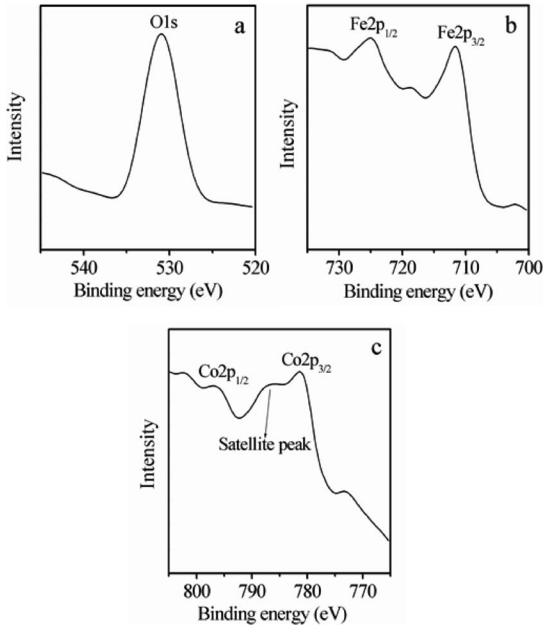

Figure 4. XPS spectra of O (a), Fe (b), and Co (c) in $CoFe_2O_4$ hollow spheres.

The magnetization curve of cobalt ferrite hollow spheres tested at 300 K is shown in Figure 5. A hysteresis loop can be observed, indicating that cobalt ferrite hollow spheres are ferromagnetic. With an increase in the external magnetic field to 15000 Oe, a saturation magnetization of 54 emu/g is achieved, which is less than that of the bulk cobalt ferrite (72 emu/g).[37] This reduction is due to surface effect and small particle size effect.[20–24] When the external magnetic field is gradually reduced to zero, due to the domain wall pinning effect, the orientation of magnetic domains remains the same and the residual magnetization is maintained, which is 18 emu/g, but it gradually decreases to zero with an increasing reverse magnetic field. In the present experiment, the coercivity of the $CoFe_2O_4$ hollow sphere is 860 Oe, which is close to that of the bulk cobalt ferrite (980 Oe).[38] In comparison to the monodispersed nanocrystals of similar size,[39] the $CoFe_2O_4$ hollow spheres show a relatively high coercivity. This is mainly due to the interaction between the nanoparticles composing the hol-

low structure.[40] Hollow spheres with such high coercivity have potential applications in such areas as drug carriers, magnetic recording, and catalysis.

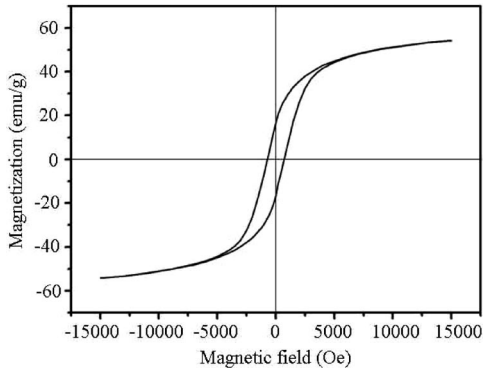

Figure 5. The hysteresis curve of $CoFe_2O_4$ hollow spheres.

Conclusions

$CoFe_2O_4$ hollow spheres with a size of 600 nm – 1 μm were synthesized by simple hydrothermal treatment and subsequent calcination. The so-prepared $CoFe_2O_4$ hollow spheres are composed of nanocrystals with an average size of ca. 30 nm. The magnetic properties show that $CoFe_2O_4$ hollow spheres have high coercivity and low saturation magnetization, which might arise from the interaction between the nanocrystals. It is expected that $CoFe_2O_4$ hollow spheres have potential applications in the areas of high-density magnetic recording materials and as drug carriers.

Experimental Section

General: All reagents were analytical grade and used as raw materials without further purification.

Synthesis of the Hollow Spheres: Glucose (15.0 g) was dissolved in deionized water (80.0 mL) and ammonium iron(II) sulfate hexahydrate $[(NH_4)_2Fe(SO_4)_2{\cdot}6H_2O]$ (7.5 mmol) and cobalt(II) sulfate heptahydrate $[CoSO_4{\cdot}7H_2O]$ (3.75 mmol) were dissolved in deionized water (10.0 mL), respectively. Then the three solutions were mixed and placed in a Teflon-lined stainless steel autoclave with a capacity of 15.0 mL, which was hydrothermally treated at 160 °C for 24 h. After cooling to room temperature, the precipitate was separated by centrifugation and washed with deionized water. The obtained precipitate was heated to 550 °C with a heating rate of 1.0 °C/min and held at that temperature for 2 h in a muffle oven to remove the carbon cores and to obtain the hollow spheres.

Spectroscopic Characterization: XRD patterns were recorded with an X-ray diffractometer (Rigaku D/Max 2200PC) with a graphite monochromator and Cu-K_α radiation (λ = 0.15418 nm). A field emission scanning electron microscope (FE-SEM, JSM-6700F), a transmission electron microscope (TEM, model H-800), and a high-resolution transmission electron microscope (HR-TEM, JEOL-2010) were used to observe the morphology and microstructure of the samples. Infrared (IR) spectra were measured with a Fourier transform infrared spectrometer (Nicolet 5DX FTIR) by using KBr pellets. The TG curve was obtained with a SDTQ600 V8.0 Build95 thermogravimetric analyzer with a heating rate of 10.0 °C/min in an air atmosphere. N_2 adsorption–desorption data were measured with a QuadraSorb SI apparatus at liquid N_2 temperature (T = –196 °C), surface area was determined by the BET (Brunauer-Emmett-Teller) method. The XPS spectrum was recorded with a PHI-5300 ESCA spectrometer (Perkin–Elmer) with its energy analyzer working in the pass energy mode at 35.75 eV, and the Al-K_α line was used as the excitation source. The binding energy reference was taken at 284.7 eV for the C1s peak arising from surface hydrocarbons. The magnetic properties were studied by Quantum Design (MPMSXL-7).

Supporting Information (see footnote on the first page of this article): The N_2 adsorption–desorption, FTIR, and TG curves of the $CoFe_2O_4$ hollow spheres.

Acknowledgments

This work was supported by the National Natural Science Foundation of China (Grant No. 20671057), the Program for New Century Excellent Talents in the University (P. R. China), and Doctoral Foundation of Shandong Province (2007BS04042).

[1] X. Xu, S. A. Asher, *J. Am. Chem. Soc.* **2004**, *126*, 7940–7945.
[2] Z. Zhong, Y. Yin, B. Gates, Y. Xia, *Adv. Mater.* **2000**, *12*, 206–209.
[3] Y. Ding, Y. Hu, X. Jiang, L. Zhang, C. Yang, *Angew. Chem. Int. Ed.* **2004**, *43*, 6369–6372.
[4] W. H. Wang, X. Ren, *J. Cryst. Growth* **2006**, *289*, 605–608.
[5] S. Kim, M. Kim, W. Lee, T. Hyeon, *J. Am. Chem. Soc.* **2002**, *124*, 7642–7643.
[6] L. Lu, G. Sun, S. Xi, H. Wang, H. Zhang, T. Wang, X. Zhou, *Langmuir* **2003**, *19*, 3074–3077.
[7] A. Imhof, *Langmuir* **2001**, *17*, 3579–3585.
[8] I. Tissot, J. P. Reymond, F. Lefebvre, E. Bourgeat-Lami, *Chem. Mater.* **2002**, *14*, 1325–1331.
[9] X. Wang, P. Hu, Y. Fangli, L. Yu, *J. Phys. Chem. C* **2007**, *111*, 6706–6712.
[10] Y. Ma, L. Qi, J. Ma, H. Cheng, *Langmuir* **2003**, *19*, 4040–4042.
[11] K. Lee, Y. Jung, S. Oh, *J. Am. Chem. Soc.* **2003**, *125*, 5652–5653.
[12] A. Khanal, Y. Inoue, M. Yada, K. Nakashima, *J. Am. Chem. Soc.* **2007**, *129*, 1534–1535.
[13] G. Liu, H. Yang, J. Zhou, S.-J. Law, Q. Jiang, G. Yang, *Biomacromolecules* **2005**, *6*, 1280–1288.
[14] J. Du, Y. Chen, *Macromolecules* **2004**, *37*, 5710–5716.
[15] X. M. Sun, Y. D. Li, *Angew. Chem. Int. Ed.* **2004**, *43*, 3827–3831.
[16] H. Wang, R. Wang, X. Sun, R. Yan, Y. Li, *Mater. Res. Bull.* **2005**, *40*, 911–919.
[17] S. H. Yu, X. Cui, L. Li, K. Li, B. Yu, M. Antonietti, H. Cölfen, *Adv. Mater.* **2004**, *16*, 1636–1640.
[18] H. S. Qian, S. H. Yu, L. B. Luo, J. Y. Gong, L. F. Fei, X. M. Liu, *Chem. Mater.* **2006**, *18*, 2102–2108.
[19] H. S. Qian, M. Antonietti, S. H. Yu, *Adv. Funct. Mater.* **2007**, *17*, 637–643.
[20] F. Caruso, M. Spasova, A. Susha, M. Giersig, R. A. Caruso, *Chem. Mater.* **2001**, *13*, 109–116.
[21] T. Hyeon, S. Lee, J. Park, Y. Chung, H. Na, *J. Am. Chem. Soc.* **2001**, *123*, 12798–12801.
[22] S. Yu, M. Yoshimura, *Adv. Funct. Mater.* **2002**, *12*, 9–15.
[23] X. Li, D. Zhang, J. Chen, *J. Am. Chem. Soc.* **2006**, *128*, 8382–8383.
[24] C. Su, H. Sheu, C. Lin, C. Huang, Y. Lo, Y. Pu, J. Weng, D. Shieh, J. Chen, C. Yeh, *J. Am. Chem. Soc.* **2007**, *129*, 2139–2146.
[25] S. Sun, H. Zeng, D. Robinson, S. Raoux, P. Rice, S. Wang, G. Li, *J. Am. Chem. Soc.* **2004**, *126*, 273–279.

[26] A. Rondinone, A. Samia, Z. Zhang, *J. Phys. Chem. B* **1999**, *103*, 6876–6880.
[27] R. Olsson, G. Salazar-Alvarez, M. Hedenqvist, U. Gedde, F. Lindberg, S. Savage, *Chem. Mater.* **2005**, *17*, 5109–5118.
[28] C. Pham-Huu, N. Keller, C. Estournès, G. Ehret, M. Ledoux, *Chem. Commun.* **2002**, 1882–1883.
[29] C. Pham-Huu, N. Keller, C. Estournès, G. Ehret, J. Grenèche, M. Ledoux, *Phys. Chem. Chem. Phys.* **2003**, *5*, 3716–3723.
[30] H. Duan, D. Wang, N. Sobal, M. Giersig, D. Kurth, H. Mŏhwald, *Nano Lett.* **2005**, *5*, 942–952.
[31] J. Bang, K. Suslick, *J. Am. Chem. Soc.* **2007**, *129*, 2242–2243.
[32] F. Caruso, C. Schuler, D. G. Kurth, *Chem. Mater.* **1999**, *11*, 3394–3399.
[33] E. Manova, B. Kunev, D. Paneva, I. Mitov, L. Petrov, *Chem. Mater.* **2004**, *16*, 5689–5696.
[34] T. Bala, C. R. Sankar, M. Baidakova, V. Osipov, T. Enoki, P. A. Joy, B. L. V. Prasad, M. Sastry, *Langmuir* **2005**, *21*, 10638–10643.
[35] X. Li, T. Lou, X. Sun, Y. Li, *Inorg. Chem.* **2004**, *43*, 5442–5449.
[36] M.-M. Titirici, M. Antonietti, A. Thomas, *Chem. Mater.* **2006**, *18*, 3808–3812.
[37] K. V. P. M. Shafi, A. Gedanken, R. Prozorov, J. Balogh, *Chem. Mater.* **1998**, *10*, 3445–3450.
[38] D. Lee, Y. Kim, Y. Kang, P. Stroeve, *J. Phys. Chem. B* **2005**, *109*, 14939–14944.
[39] K. Mooney, J. Nelson, M. Wagner, *Chem. Mater.* **2004**, *16*, 3155–3161.
[40] Y. Wang, Q. Zhu, H. Zhang, *J. Mater. Chem.* **2006**, *16*, 1212–1214.

Received: April 28, 2008
Published Online: July 25, 2008

